

## ARTICLES

## 500-MeV pion single-charge exchange on deuterium

R. J. Peterson, J. Ouyang,\* and S. Høibråten†

*Nuclear Physics Laboratory, University of Colorado, Boulder, Colorado 80309*

L. B. Weinstein

*Department of Physics, Old Dominion University, Norfolk, Virginia 23529*

(Received 10 February 1995)

Measurements of spectra from the  ${}^2\text{H}(\pi^-, \pi^0)$  reaction with a 500 MeV beam have been made from near zero degrees to 90 degrees. A peak corresponding to breakup or quasielastic scattering is observed, and its width, maximum, and differential cross section are reported. Peak shape determinations were also made with the  ${}^2\text{H}(\pi^+, \pi^0)$  reaction. Results are compared to recent pion charge exchange data on deuterium at lower pion beam energies. A simple impulse approximation calculation accounts for the data at all angles.

PACS number(s): 25.80.Gn, 25.10.+s

## I. INTRODUCTION

Pion reactions with deuterons provide one view of the most elementary strong interaction, and have been extensively studied [1]. The reaction with the smallest data set has been pion single charge exchange (SCX), leading to the unbound final state of two identical nucleons. A recent experiment has measured new cross sections for SCX over a wide angular range for three negative pion beam energies 164, 263, and 371 MeV [2]. We report here a measurement of the spectra over a wide angular range with 500 MeV negative pions, with some data also at 400 MeV, and with spectral shapes also measured over a wide range of angles for 500 MeV positive pions [3]. These data cover much the same range of momentum transfers as do the data from Ref. [2]. The important small reaction angles are covered with all four pion beam energies.

Reactions on deuterium are much like those on free nucleons, except at small scattering angles with small momentum transfers  $q$ . Final states of two identical nucleons with the same spin as the target are Pauli blocked, and not available to the recoiling nucleons, and spin changing cross sections vanish at zero degrees. The pion SCX data of Ref. [2] included very small scattering angles by placing the detector directly in the low intensity beam. In the present work we reach small scattering angles by detecting the two-photon decay of the  $\pi^0$  at angles symmetric about zero degrees. Other placements of the two-element spectrometer allowed data to be recorded

out to angles of 90°.

Pion breakup scattering without charge exchange (NCX) has also been measured on deuterium [4–6], but there are important differences in SCX. In charge exchange the final identical nucleons are not able to interact through the strongly attractive  ${}^3S_1$  coupling, and so nuclear final state interactions are weaker in SCX than in NCX. Absorption of the pion on an isospin one pair of identical particles is observed to be much weaker than on isospin-zero pairs [7], and so the truncation of the multiple scattering series can occur more promptly by absorption in NCX than in SCX. It is useful to note that the 500 MeV beam energy provides a prominent minimum in the  $\pi$ -deuteron total cross section [8] or a maximum in the mean free path. The 500 MeV beam energy is also the maximum for which a recent phase shift analysis of  $\pi$ -deuteron elastic scattering has been carried out [9]. We emphasize the use of the  ${}^2\text{H}(\pi^-, \pi^0)$  reaction because of the lack of Coulomb interactions in the final three-body state. Two charged particles are in the final state for the SCX data studied by the  ${}^2\text{H}(\pi^+, pp)\pi^0$  reaction [10].

## II. METHODS

We performed the experiment at LAMPF using 400 and 500 MeV pion beams from the  $P^3$  channel. The  $\pi^+$  beam contained protons as well, and their intensity was determined by particle identification of a small fraction of the beam in a sampling grid scintillator [11]. An ion chamber downstream from the scattering target was used for relative normalization of the beams. The LAMPF neutral pion spectrometer consists of two crates, each containing an array of lead glass converters, wire chambers to localize the showers associated with converted photons, and a lead glass calorimeter. The total energies

\*Present address: Department of Physics, Boston University, Boston, MA 02215.

†Present address: FFIVM, Kjeller, Norway.

of neutral pions are identified through their 98.8% decay into two photons, with the opening angle of the two photons as the principal determinant of the total energy, and only a weak dependence on the total energy seen by the calorimeter [12].

We determined the absolute efficiencies of the spectrometer by measuring  $H(\pi^-, \pi^0)$  cross sections using  $CH_2$  targets and subtracting the carbon background. Carbon charge exchange spectra from this experiment are presented elsewhere [13]. Cross sections for the free pion SCX were taken from the phase shift compilation of Ref. [14], using solution FA93. We measured  $\pi^-$  SCX cross sections for deuterium using solid targets of  $CD_2$  with the same geometry and counting rate as for the C and  $CH_2$  targets. Very few events were seen with empty target frames, but these spectra were also subtracted for our final results. Cross sections from the  $2.38 \pm 0.4\%$   $CH_2$  content of the  $CD_2$  target were subtracted from the  $CD_2$  cross sections.

The spectrometer was set to receive central scattering at angles of  $0^\circ$ ,  $30^\circ$ ,  $50^\circ$ ,  $70^\circ$ , and  $88.8^\circ$  in the laboratory. Events in the large angular acceptance were sorted into angular bins of  $\pm 3.5^\circ$  centered at these central angles, except at the largest angle setting where the central angle was taken to be  $90^\circ$ , and the forward angles where events were taken centered about  $6.6^\circ$  with a  $+4^\circ$ ,  $-3^\circ$  bin and from  $0^\circ$  to  $3.5^\circ$  centered at  $2.3^\circ$ . Energy bins shown in the present work are 9 MeV wide, although fitting was carried out with 3 MeV bins. The relative spectrometer acceptance was computed with the Monte Carlo program PIANG [12].

Negative pion SCX cross sections on deuterium were then determined directly by comparison to the SCX cross sections on hydrogen. Since beam rates and dead times were much different for the more intense  $\pi^+$  beam, we do not report cross sections for this beam sign.

Figure 1 shows doubly differential SCX cross sections for 500 MeV negative pions on deuterium, after subtraction of the carbon events with matching runs. The vertical dotted lines show the energies where the free SCX is expected and observed. These free SCX spectra show peaks with widths in agreement with the expectations of the PIANG modeling, and are listed in Table I. The deuteron spectra show peaks coinciding with the free peaks. These are from the quasifree SCX scattering on one of the nucleons in the target.

### III. RESULTS

We fit these doubly differential spectra with a peak shape formed by two half Gaussians, with different widths on the two sides. A quadratic background was estimated and subtracted, as shown in the figure. The resulting maxima are listed in Table I. The measured full width at half maximum of the H spectrum corresponding to each  ${}^2H(\pi^-, \pi^0)$  and  $(\pi^+, \pi^0)$  spectrum was subtracted in quadrature to give the full widths at half maximum for the deuteron listed in Table I. Runs with the two beam signs were taken without moving the spectrometer. These maxima and widths may be taken to

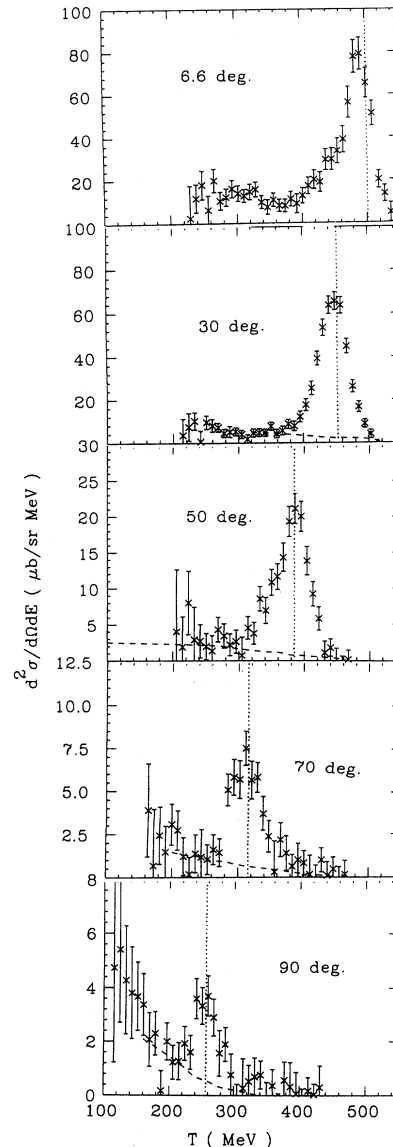


FIG. 1. Doubly differential cross sections in the laboratory reference frame are shown for neutral pions resulting from 500 MeV negative pions on deuterium, obtained by subtracting C spectra from those for  $CD_2$ . Energy bins are 9 MeV and angle bins are  $\pm 3.5^\circ$  for each sample shown, except for the smallest angles. The vertical dotted lines locate free SCX in each case. The quadratic backgrounds shown were used to integrate these spectra for the singly differential cross sections of the quasielastic peaks.

represent our peak shapes for both beam signs.

The widths and maxima for each angle bin of the experiment, including those not shown in the spectra of Fig. 1, are plotted in Fig. 2. The energy maxima are shown relative to those observed for free proton SCX. Instead of an angle scale, the laboratory-frame three-momentum transfer  $q$  to a single struck free nucleon is used in Fig. 2. This presents easy comparison to the data for 400 MeV  ${}^2H(\pi^-, \pi^0)$  taken with a single angle setting of  $62.6^\circ$  to

TABLE I. Fitted values for the widths, maxima, and differential cross sections of the experiment are listed. The fitted full width at half maximum (FWHM)  $\Gamma$  for H was subtracted in quadrature from those fit to the  $^2\text{H}$  spectra to determine the values of  $\Gamma_D$  below. All values are given in the laboratory frame. With 400 MeV  $\pi^-$  we obtain  $\Gamma_D$  of 38.3(3), 39.4(3), and 36.0(7) MeV at angles of 54.0°, 62.7°, and 71.5°. The corresponding peak maxima are at 297.8(3.5), 276.0(3.1), and 254.8(5.1) MeV, with cross sections of 1.1(0.2), 0.80(0.2), and 0.30(0.1) mb/sr. All angle bins are  $\pm 3.5$  MeV wide except for the most forward angle points.

$\Theta$ (deg)	$q$ (MeV/c)	$\Gamma_H$ (MeV)	500 MeV $\pi^-$			500 MeV $\pi^+$	
			$\Gamma_D$ (MeV)	Maximum (MeV)	$d\sigma/d\Omega$ (mb/sr)	$\Gamma_D$ (MeV)	Maximum (MeV)
2.3	25.0				2.34 (0.3)		
6.6	71.7				5.01 (0.45)		
24.1	256.0	38.1	40.8	468.5(1.6)	6.77(0.66)	28.5	460.1(2.3)
30.0	314.0	41.4	36.7	449.3(1.9)	3.77(0.35)	24.3	449.7(2.0)
36.1	371.0	36.5	45.6	433.1(2.9)	3.36(0.5)	38.8	434.6(3.1)
43.6	437.0	39.3	43.2	403.6(4.0)	1.75(0.2)	36.7	406.3(3.8)
50.0	489.0	37.6	47.3	391.4(3.3)	1.24(0.2)	34.4	383.8(4.7)
56.4	536.0	33.6	42.0	380.1(4.9)	0.62(0.1)	34.3	354.1(6.3)
63.4	584.0	34.2	56.1	340.8(7.7)	0.53(0.1)	37.8	340.1(4.6)
70.0	625.0	32.8	40.9	305.2(8.2)	0.36(0.08)	50.7	307.6(5.3)
76.6	662.0	22.1	37.5	293.6(6.0)	0.32(0.1)	41.4	290.7(7.6)
83.2	694.0	26.9	57.5	274.2(8.0)	0.25(0.07)	30.3	274.4(7.5)
90.0	725.0	27.5	37.7	254.2(9.4)	0.15(0.05)	27.2	251.1(4.5)

attain the same  $q$  as for 500 MeV beam at 50°. The energy difference from free scattering is seen to be small and nearly constant. At the smallest angle there could be a significant difference between the shifts with 500 MeV  $\pi^+$  and  $\pi^-$ .

The widths plotted in Fig. 2 are nearly constant, and appear to differ at small angles for  $\pi^+$  and  $\pi^-$ . The small  $\text{CH}_2$  content in the  $\text{CD}_2$  target would make the  $\pi^-$  spectra slightly narrower, opposite to the effect seen. The momentum transfer dependence of the widths for pion SCX differs significantly from the dependence of the widths from quasielastic electron scattering on deuterium. These ( $e, e'$ ) widths increase approximately linearly with  $q$ , with  $\Gamma \simeq 80$  MeV  $q/m$ , up to four-momentum transfers  $Q^2=1.75$  ( $\text{GeV}/c$ )<sup>2</sup> [15–19], whereas the pion SCX peak widths seem to be independent of  $q$ .

Singly differential cross sections were determined by the areas of the fits to the peak, such as in Fig. 1, only for  $\pi^-$  to maintain a reliable absolute normalization. These are plotted in Fig. 3, with a laboratory angle scale. The three points from a single spectrometer setting at 400 MeV are also shown, scaled down by a factor of 10. Uncertainties include the counting statistics for the subtracted  $^2\text{H}$  and the normalizing subtracted H spectra and the fitting uncertainties, including that for the background. The dashed lines are the free SCX cross sections with the same angle binning from SAID [14]. At large scattering angles these agree with the deuteron points, as expected for truly free SCX on the proton in the target. No significant attenuation of the cross sections due to the other nucleon is apparent.

At small scattering angles the SCX cross sections show the effect of the Pauli blocking due to the spectator neutron in the final state. This feature is also prominent for

SCX at 500 MeV on complex nuclei [20]. It is an advantage of the  $\pi^0$  detector system that these small angles are readily accessible.

These same 500 MeV cross sections are compared to the data of Ref. [2] on a scale of the momentum transfer to a free struck nucleon in Fig. 4. All four data sets show a decrease of small angles. The dashed curves show the free SCX cross sections at each energy. At 164 MeV the deuteron cross sections lie below this curve everywhere, due to the strong effect of distortions and absorption at this resonant energy. This is in agreement with the calculations of Garcilazo compared to 164 MeV data taken some years ago [21]. Comparisons are shown in Ref. [21].

Differential cross sections for a spin excitation of the target already satisfy the Pauli principle. These cross sections from SAID [14] are shown by the dotted curves for the four beam energies in Fig. 4. These must vanish at zero degrees for the spin-zero projectile. Differential cross sections without a spin transfer are Pauli blocked at small  $q$ . We model this by taking the simplest deuteron wave function, proportional to  $e^{-\gamma r}$ , suited to large radii or small  $q$ , with  $\gamma$  determined from the binding energy to be  $0.2315$  fm<sup>-1</sup>. The density this provides was Fourier transformed to a density of momentum states, and joint occupation of two such distributions separated by  $q$  gives a multiplicative blocking factor given by  $N_{\text{BF}} = 1 - \frac{1}{(1+x^2)^2}$ , with  $x = q/4\gamma$ . Free nonspin cross sections multiplied by this factor are shown in Fig. 4. All predicted cross sections have been binned in scattering angle as the data were provided, with a “10° resolution” for 164, 263, and 371 MeV [2]. This angle binning is particularly vital at the small reaction angles. These curves, using only what must be true for the deuteron, closely account for the

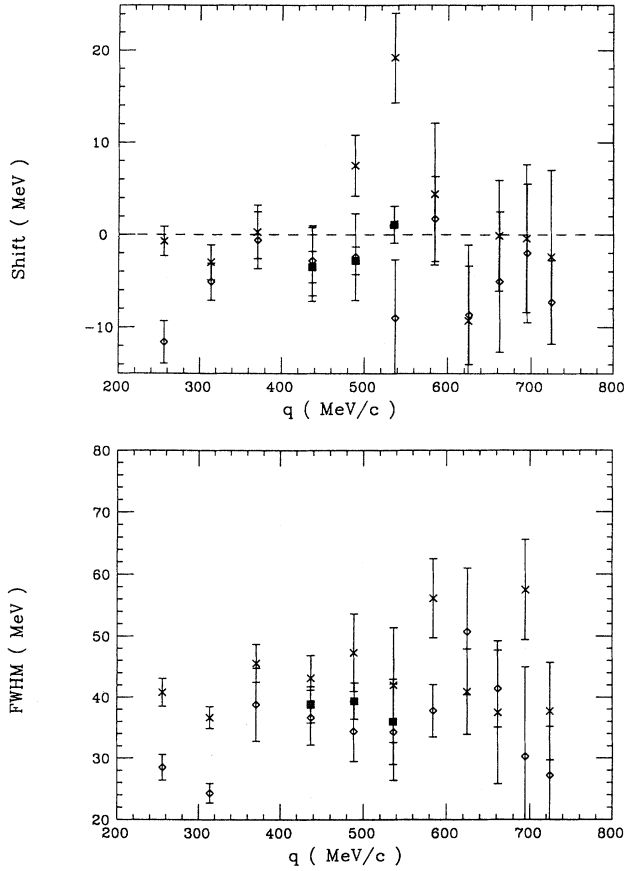


FIG. 2. Shifts of the maximum of the fitted quasielastic peaks from the values for free SCX are plotted as a function of the laboratory momentum transfer to a free nucleon. Crosses are for 500 MeV  $\pi^-$ , diamonds are for 500 MeV  $\pi^+$ , and squares are for 400 MeV  $\pi^-$ . The deuteron binding energy would lead to an expected shift at  $-2.2$  MeV. The fitted full widths at half maximum of the quasielastic peaks are also shown, after subtraction in quadrature of the width of the corresponding free SCX.

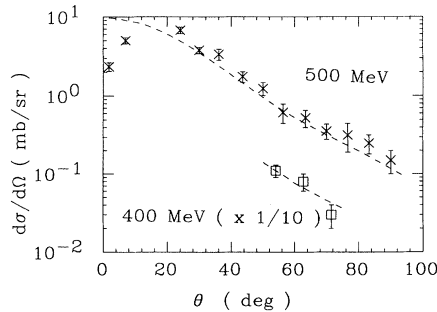


FIG. 3. Singly differential cross sections for 400 MeV and 500 MeV pion quasielastic SCX on deuterium are shown in the laboratory reference frame. Dashed lines show the free nucleon SCX cross sections [14].

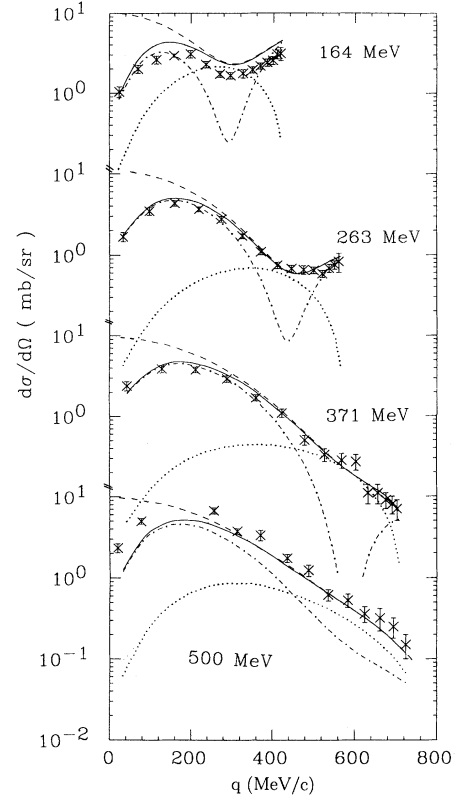


FIG. 4. The differential cross sections for 500 MeV negative pions are plotted against the free nucleon laboratory momentum transfer scale to compare with the data of Ref. [2]. Dashed lines show the free nucleon SCX cross sections [14], while the free spin transfer cross sections are used to form the dotted curves. Dot-dashed curves Pauli block the free nonspin cross sections by the expression in the text. The solid curves are the sums of these expectations. All predicted curves have been collected into the same angle bins as the data.

shapes of the SCX cross sections at all angles for all four beam energies. At 164 MeV the data lie below the solid curve, because of shielding of the proton by the neutron with the large resonant cross section. In addition to the uncertainties shown, the three lower beam energies provide a 5% systematic uncertainty in magnitude [2], while a 9% uncertainty in magnitude is estimated at 500 MeV [3].

The eikonal model has been effective for estimating the magnitudes of pion SCX cross sections for heavy nuclei and high energies [22]. Here, the simple exponential model for the deuteron density is used, with the free  $\pi^-$ -neutron total cross section shielding the  $\pi^-$ -proton SCX cross section half the time. The effective number of protons available in this calculation is 0.90 at 164 MeV and unity for the higher beam energies. If the curves in Fig. 4 for 164 MeV are multiplied by 0.90, they will more closely match the magnitude, as well as the shape, of the SCX data.

#### IV. CONCLUSIONS

We have measured SCX double- and single-differential cross sections for the neutral pions from SCX of  $\pi^-$  on deuterium at 500 MeV to extend the range of studies recently reported in Ref. [2]. Data for yet lower energies of 65 and 98.5 MeV have recently been taken and are being analyzed [23]. This now rather complete data set greatly expands the base upon which theories of this elementary reaction system can be based. The plane wave impulse approximation, blocked by the simplest features

of the target deuteron, comes remarkably close to the data. Comparison also to a number of electron scattering deuteron breakup measurements in this same range of momentum transfers will make a consistent description particularly interesting. Complete data tables for inclusive spectra from the present experiment are available in a thesis [3] and in tables [24].

We wish to thank those who assisted in the experiment that included the deuterium data and A. Saunders for help with MATHEMATICA.

- 
- [1] H. Garcilazo and T. Mizutani, *PiNN Systems* (World Scientific, Singapore, 1990).
- [2] H. T. Park, *Phys. Rev. C* **51**, 1613 (1995).
- [3] J. Ouyang, Ph.D. thesis, University of Colorado, Los Alamos Report No. LA-12457-T, 1992.
- [4] M. A. Khandaker, M. Doss, I. Halpern, T. Murakami, D. W. Storm, D. R. Tieger, and W. J. Burger, *Phys. Rev. C* **44**, 24 (1991).
- [5] W. List, E. T. Boschitz, H. Garcilazo, W. Gyles, C. R. Otterman, R. Tacik, M. Wessler, U. Wiedner, and R. R. Johnson, *Phys. Rev. C* **37**, 1587 (1988).
- [6] Y. D. Bayukov, V. B. Fedorov, V. M. Kolybasov, V. G. Ksenzov, G. A. Leskin, V. L. Stolin, and L. S. Vorobyev, *Nucl. Phys.* **A282**, 389 (1977).
- [7] D. Ashery *et al.*, *Phys. Rev. C* **30**, 946 (1984).
- [8] A. A. Carter *et al.*, *Phys. Rev.* **168**, 1457 (1968).
- [9] R. A. Arndt, I. I. Strakovsky, and R. L. Workman, *Phys. Rev. C* **50**, 1796 (1994).
- [10] R. Tacik, E. T. Boschitz, W. Gyles, C. R. Otterman, M. Wessler, U. Wiedner, H. Garcilazo, and R. R. Johnson, *Phys. Rev. C* **42**, 1846 (1990).
- [11] J. D. Bowman *et al.*, *Nucl. Instrum. Methods A* **349**, 32 (1994).
- [12] H. Baer *et al.*, *Nucl. Instrum. Methods* **180**, 445 (1981).
- [13] J. Ouyang, S. Høibråten, and R. J. Peterson, *Phys. Rev. C* **48**, 1074 (1993).
- [14] R. A. Arndt, Z. Li, L. D. Roper, R. L. Workman, and W. M. Ford, *Phys. Rev. D* **43**, 2131 (1991); computer code SAID, Virginia Polytechnic Institute and State University, Blacksburg, VA.
- [15] B. Quinn *et al.*, *Phys. Rev. C* **37**, 1609 (1988).
- [16] E. Hummel and H. J. Tjon, *Phys. Rev. C* **49**, 21 (1994).
- [17] B. Parker, R. S. Hicks, A. Hotta, R. L. Huffman, G. A. Peterson, M. A. Plum, P. J. Ryan, and R. P. Singhal, *Phys. Rev. C* **34**, 2354 (1985).
- [18] L. Stuart, Ph.D. thesis, University of California, Davis, Lawrence Livermore National Laboratory Report No. UCRL-LR-110897, 1992.
- [19] J. R. Harrington *et al.* (unpublished); R. Ent (private communication).
- [20] R. J. Peterson *et al.*, *Phys. Lett. B* **297**, 238 (1992).
- [21] H. Garcilazo, *Phys. Rev. C* **47**, 957 (1993).
- [22] J. Ouyang, S. Høibråten, and R. J. Peterson, *Phys. Rev. C* **47**, 2809 (1993).
- [23] M. V. Keilman (private communication).
- [24] See AIP Document No. PAPS PRVCA-52-33-5 for 5 pages of tabulated cross sections. Order by PAPS number and journal reference from American Institute of Physics, Physics Auxiliary Publication Service, Carolyn Gehlbach, 500 Sunnyside Boulevard, Woodbury, New York 11797-2999; e-mail: janis@aip.org. The price is \$1.50 for microfiche, or \$6.35 for photocopies. Airmail additional. Make check payable to American Institute of Physics. This material appears in the monthly *Current Physics Microfilm* edition of all journals published by AIP, on the frames following this paper.